

Join us at

# INTERSECTIONS

~~May 30 - June 5, 2022~~

Lake Buena Vista, Fla

August 29-  
September 4

## Recent STAR Results on the Unpolarized Light Quark Flavor Structure at RHIC

Jae D. Nam  
Temple Univ.



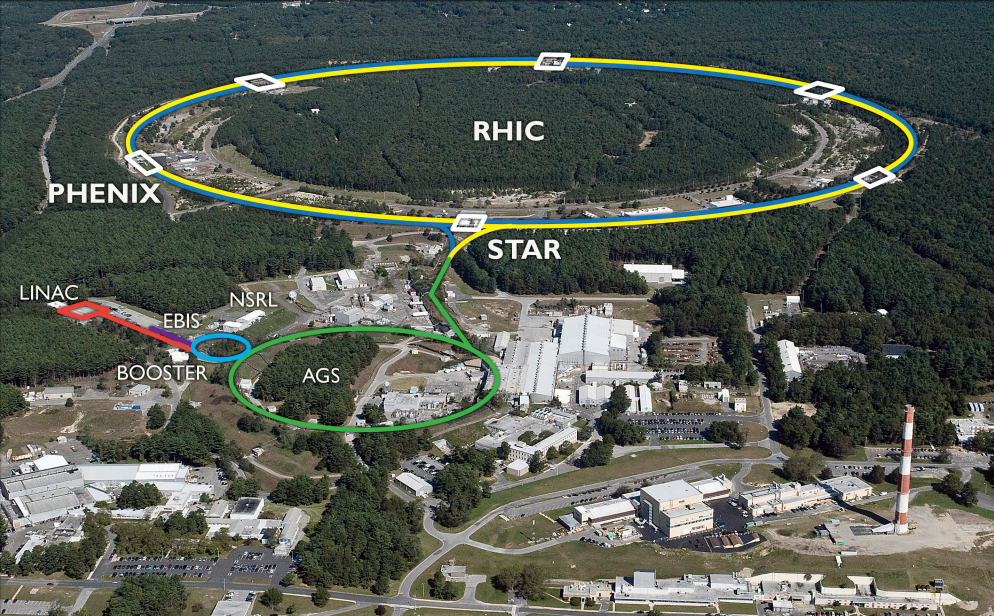
8/30/22

Jae D. Nam

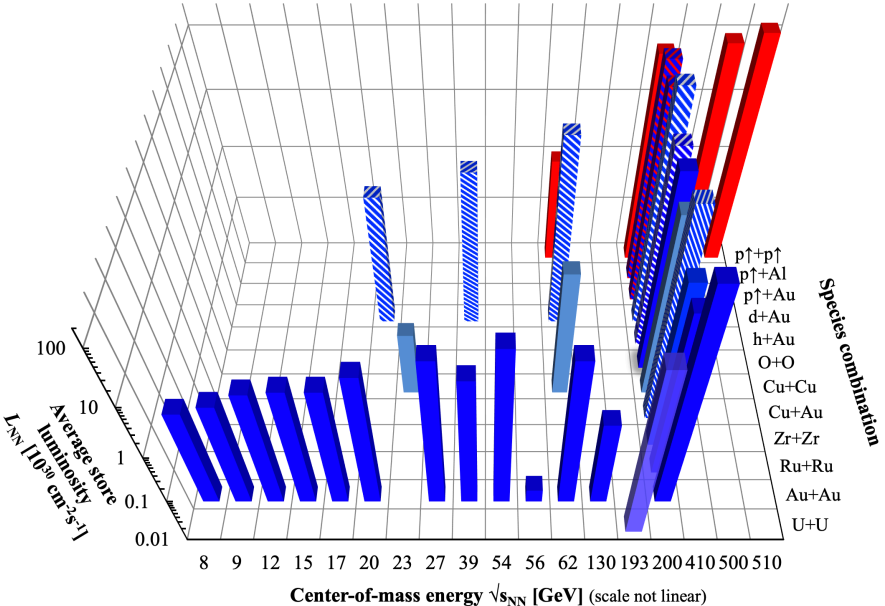
1



# Relativistic Heavy Ion Collider



RHIC energies, species combinations and luminosities (Run-1 to 22)



- RHIC continues to serve as the world's first and only polarized  $pp$  collider.
- Features  $pp$  collisions at  $\sqrt{s} = 500/510 \text{ GeV}$  and  $\sqrt{s} = 200 \text{ GeV}$ .
- $pA/AA$  collisions at  $\sqrt{s_{NN}} = 10\sim 200 \text{ GeV}$ .
- At RHIC, protons can be polarized either:
  - Longitudinally (along the direction of the beam)
    - Proton spin composition
  - Transversely (perpendicular to the beam)
    - 3D image of the proton
  - Or can be unpolarized (if we choose not to look at the polarization)
    - **Parton distribution functions**
    - Non-linear gluon effects

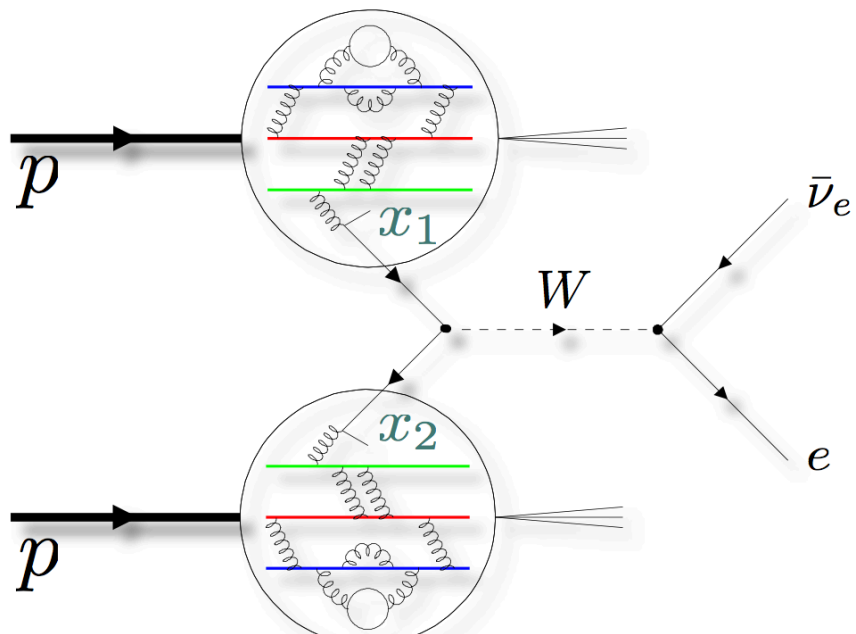


# Measurements of PDFs at RHIC

- Drell-Yan type measurements:

$$d\sigma \sim \sum_{1,2} [f_1(x_1)\bar{f}_2(x_2) + \bar{f}_1(x_1)f_2(x_2)] \otimes d\hat{\sigma}_{1,2}$$

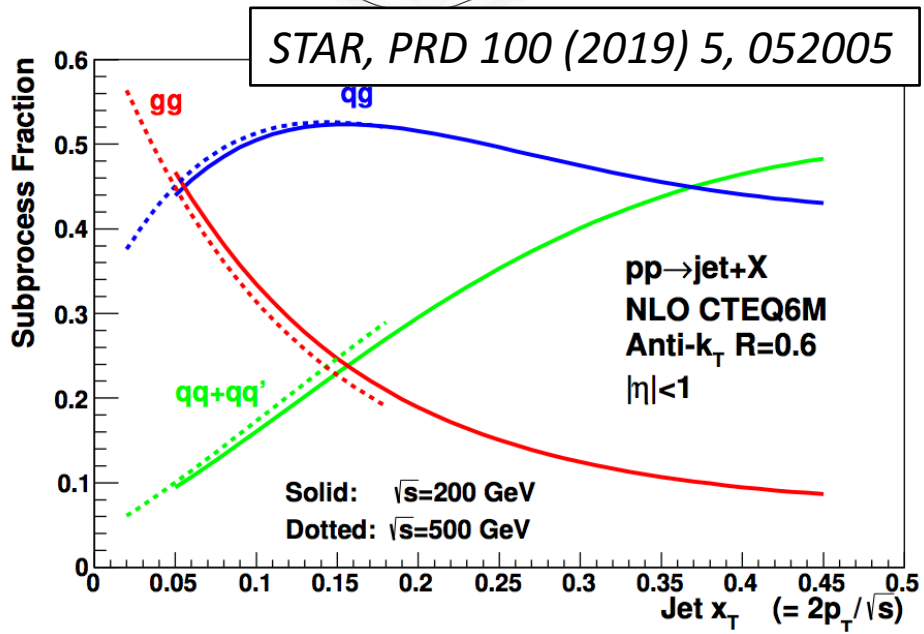
- Sensitive to both quark/anti-quarks in the proton.
- Simple final state of charged leptons: No dependency on FFs.



- Inclusive Jet measurements:

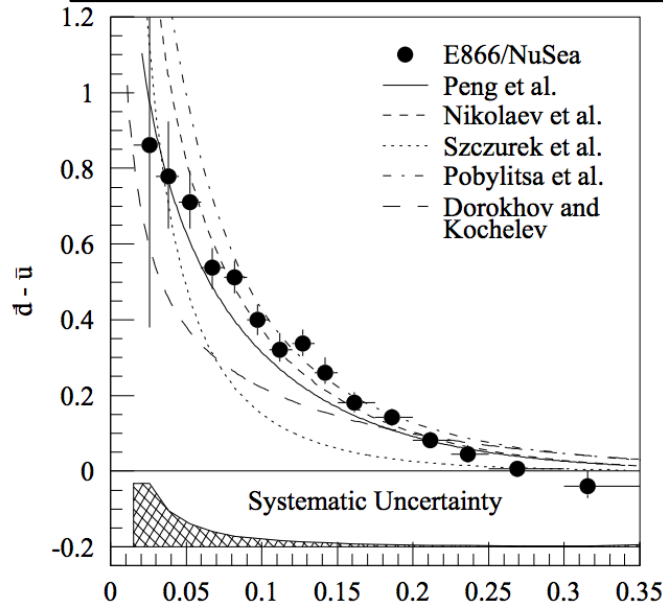
$$d\sigma \sim \sum_{1,2} f_1(x_1, Q_1^2)f_2(x_2, Q_2^2) \otimes d\hat{\sigma}_{1,2}$$

- Jets in STAR kinematics sensitive to gluons in the proton.
- Many jet studies have been already produced from STAR with polarized beams.
- Different CoM energy / jet topology provide additional information of the initial state proton

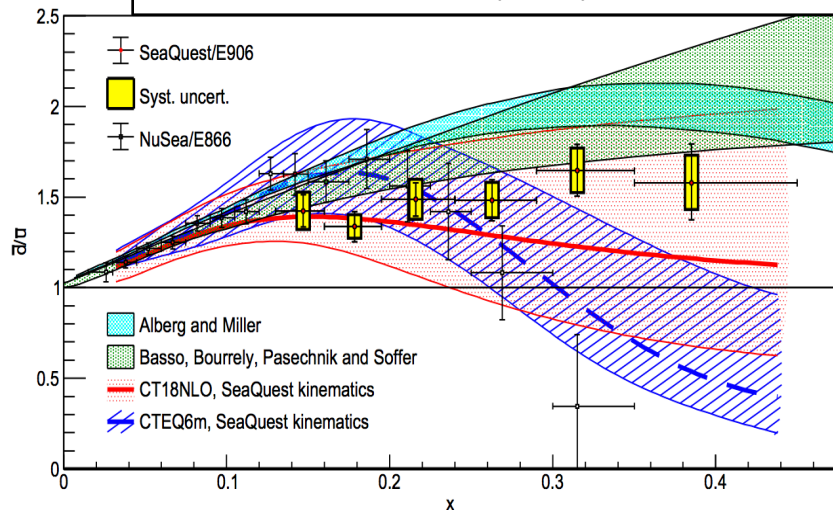


# $\bar{d}/\bar{u}$ asymmetry

NuSea, Phys.Rev.D 64 (2001) 052002



SeaQuest, Nature 590 (2021) 7847, 561-565



- While the valence quark ( $d, u$ ) structure of the proton is well determined, the anti-quark counter part ( $\bar{d}, \bar{u}$ ) is much less constrained.
- Non-diminishing asymmetry between the anti-quarks in the proton sea  $\bar{d}, \bar{u}$  is a purely non-perturbative phenomenon.
- The anti-quark ratio  $\bar{d}/\bar{u}$  is typically measured in Drell-Yan type experiments with deuterons.
- Inconsistencies among these measurements have been found, especially in the proton momentum fraction range  $x > 0.2$ .
- $W$  measurements at RHIC may provide some insight around the region of conflict.

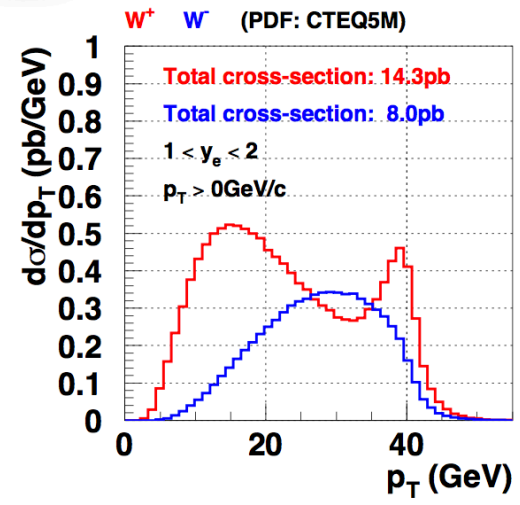
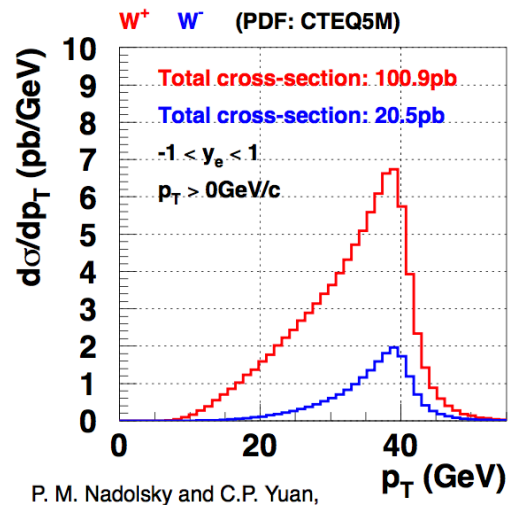
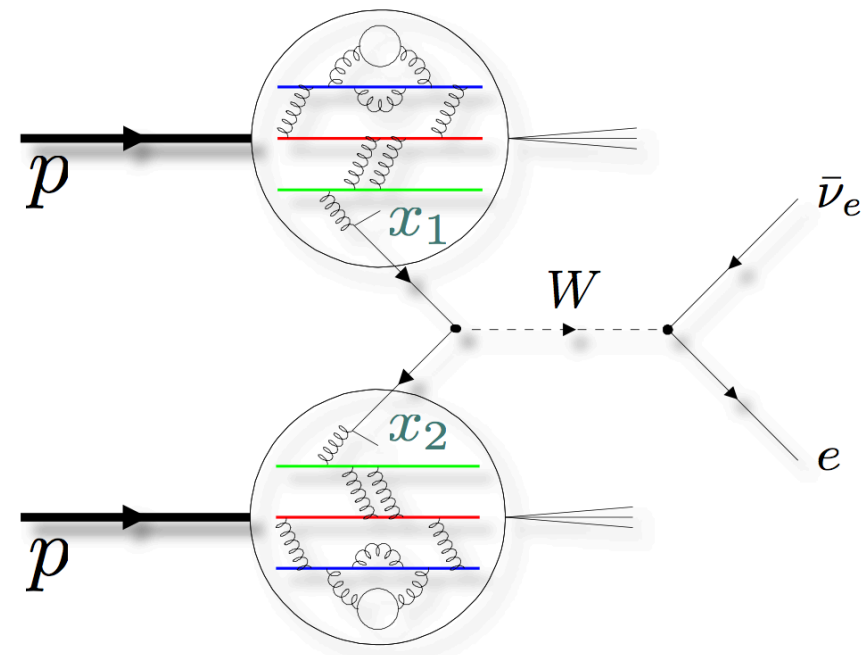
# W production in pp collisions

- $W^\pm$  cross sections at LO
  - $d\sigma^{W^+} \propto u(x_1)\bar{d}(x_2) + u(x_2)\bar{d}(x_1)$
  - $d\sigma^{W^-} \propto \bar{u}(x_1)d(x_2) + \bar{u}(x_2)d(x_1)$

$$\rightarrow R_W = \frac{\sigma^{W^+}}{\sigma^{W^-}} \sim \frac{u(x_1)\bar{d}(x_2) + u(x_2)\bar{d}(x_1)}{\bar{u}(x_1)d(x_2) + \bar{u}(x_2)d(x_1)}$$

- At LO, momentum scale set by the W mass,  $Q^2 \sim M_W^2$ .
- Leptonic decay via  $W \rightarrow ev$ 
  - $\frac{d\sigma(W^\pm \rightarrow ev)}{dp_{T,e}^2} \propto \frac{(1 \pm \cos \theta)^2}{M_W \cos \theta}$
  - $p_{T,e} \sim \frac{M_W}{2} \sin \theta$
  - Jacobian peak at  $p_{T,e} \sim M_W/2$
  - $y_e \sim y_W + \frac{\ln 1 + \cos \theta}{\ln 1 - \cos \theta}$
  - Charge discrimination as a function of  $y_e$ .

- Key features in experiment
  - High  $p_T$  electron.
  - Electron/Hadron discrimination needed.
  - Large imbalance in  $p_T$  in detector due to  $\nu$ .

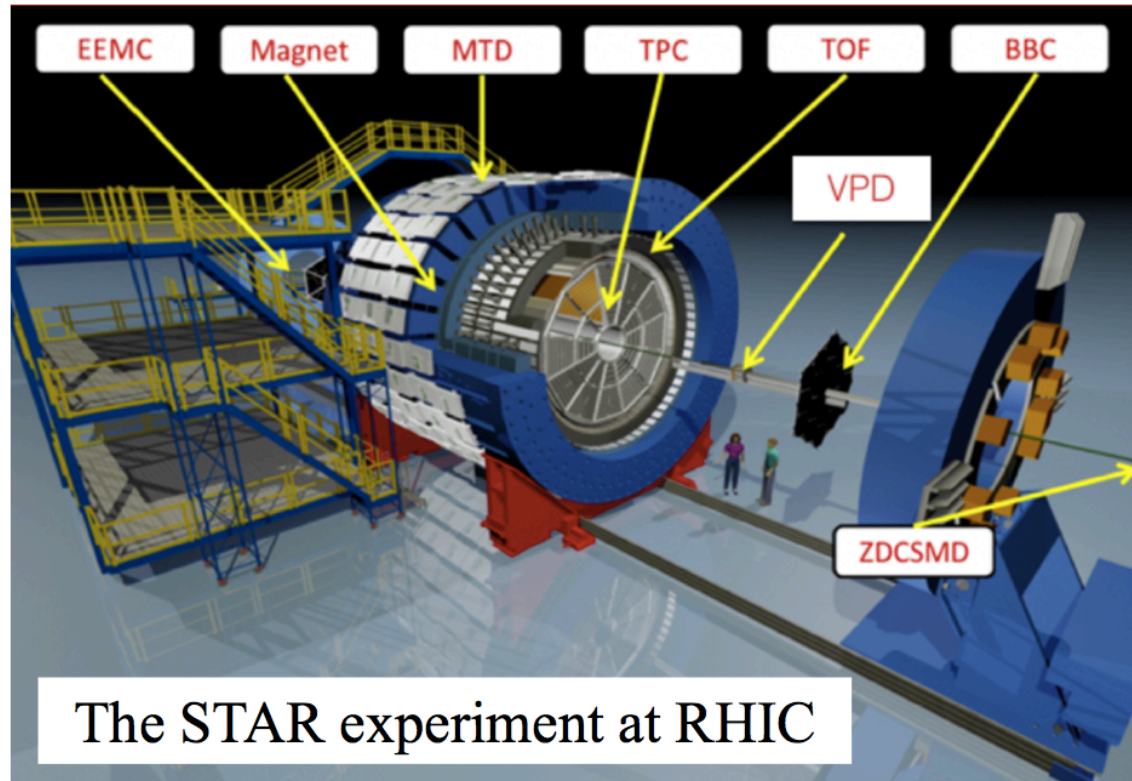


P. M. Nadolsky and C.P. Yuan,  
 Nucl.Phys. B666 (2003) 31.  
 Jae D. Nam



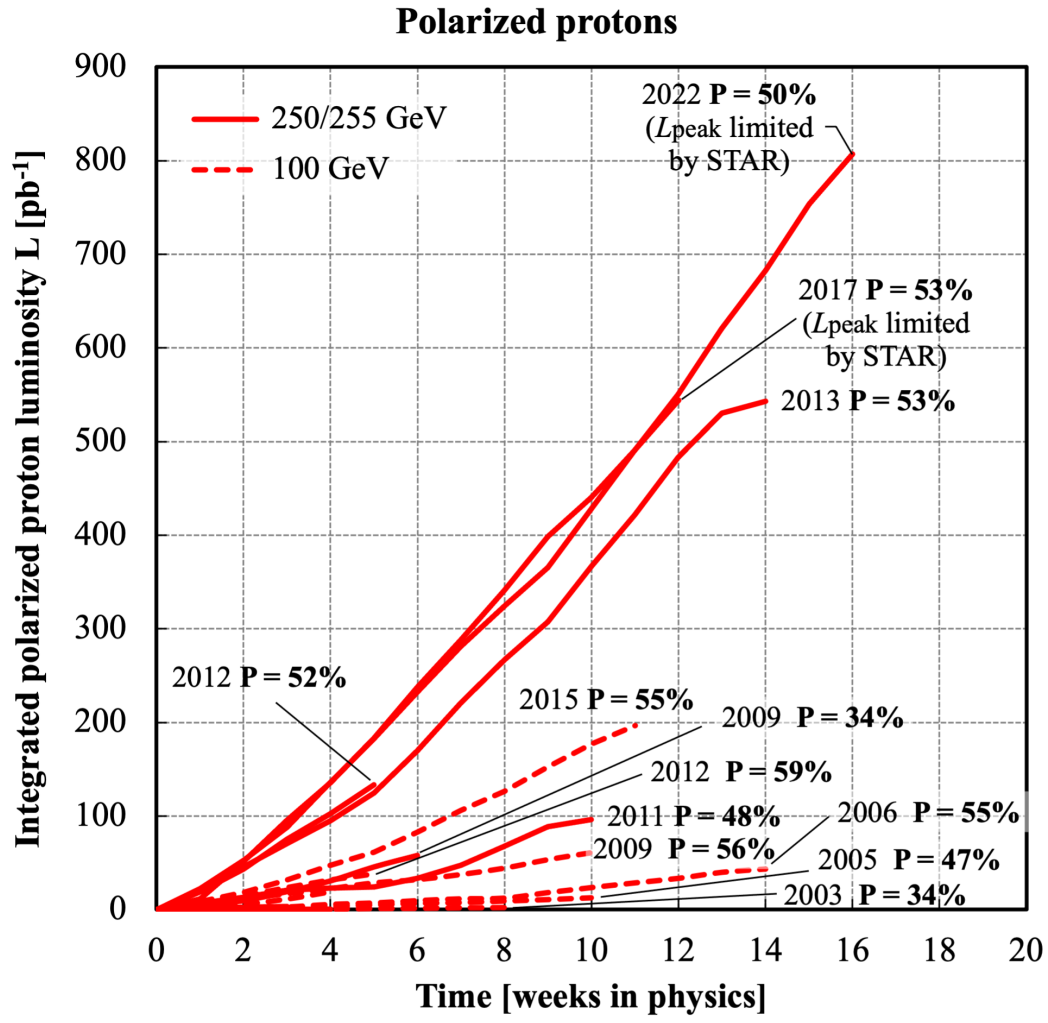
# Solenoid Tracker At RHIC (STAR)

- For measurements of  $W$  bosons, it is important to achieve near  $4\pi$  detector acceptance.
- Time Projection Chamber (TPC)
  - Acceptance of  $|\eta| < 1.3$ .
  - Provides tracking & PID.
- Electro-Magnetic Calorimeter
  - Barrel (BEMC):  $|\eta| < 1$ .
  - Endcap (EEMC):  $1 < \eta < 2$ .
  - Assists in electron/hadron discrimination.
  - Assists in electron charge discrimination.
- Luminosity monitoring & Vertexing
  - Beam-Beam Counter (BBC)
  - Zero Degree Counter (ZDC)
  - Vertex Position Detector (VPD)



- The  $W$  bosons detected in the combined TPC + BEMC (barrel region) arise from a kinematic region of  $0.1 < x < 0.3$ .
- EEMC provides coverage in the intermediate region  $1 < \eta < 2$ , extending the kinematic reach to  $0.06 < x < 0.4$ .

# RHIC $pp$ Run Overview

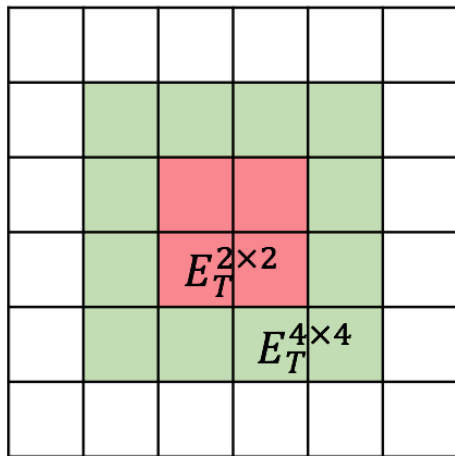


Run	$\sqrt{s}$ (GeV)	$L$ ( $pb^{-1}$ )
2009	500	10
2011	500	25
2012	510	75
2013	510	250
2017	510	350
2022	510	400 (estimate)

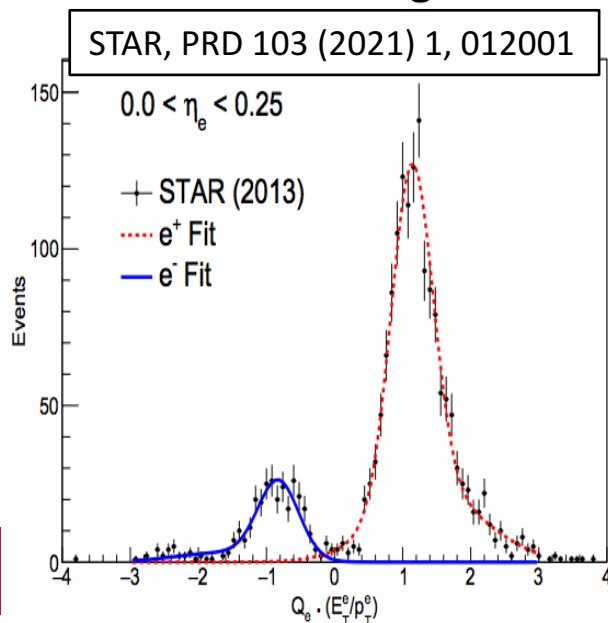
- $L \sim 700 + 400 pb^{-1}$  of  $pp$  collisions with sufficiently high  $\sqrt{s}$  has been collected at STAR.
  - Initial measurement based on Run 2009 with  $L \sim 10 pb^{-1}$ . (STAR, PRD 85 092010)
  - Follow up study with Run 2011-2013 with  $L \sim 350 pb^{-1}$  has been published. (STAR, PRD 103,012001)
  - Preliminary study based on Run 2017 with  $L \sim 350 pb^{-1}$ .
  - New dataset with  $L \sim 400 pb^{-1}$ .



# $W$ tagging in the barrel ( $|\eta_e| < 1$ )

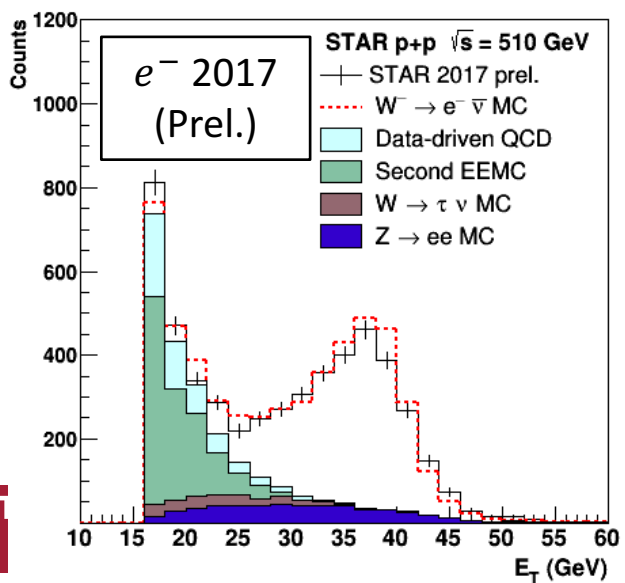
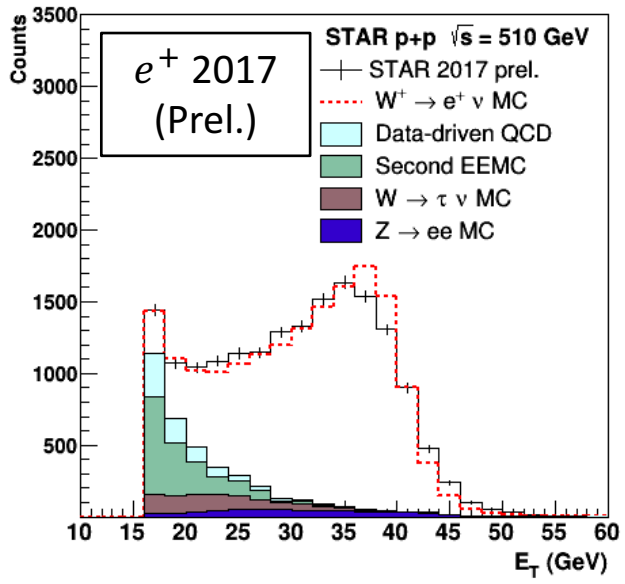


TPC track extrapolated to BEMC tower grid



- $W$  bosons that undergo the leptonic decay process,  $W \rightarrow e\nu$ , are tagged.
- Imbalance in  $p_T$  due to the missing neutrino. High  $\vec{p}_{T,bal}$  ( $= \vec{p}_{T,e} + \Sigma \vec{p}_{T,recoil}$ ) events are selected.
- Unlike hadrons, electrons deposit their energy in a highly concentrated region in the EMC. This isolated electron energy deposit is quantified with  $E_T^{2 \times 2} / E_T^{4 \times 4}$ .
- Charge separation from TPC + EMC ( $Q_e \times E_T / p_T$ ).
- Although not in this measurement, full  $W$  kinematics can be reconstructed.
  - Used for measurements of Sivers effect.

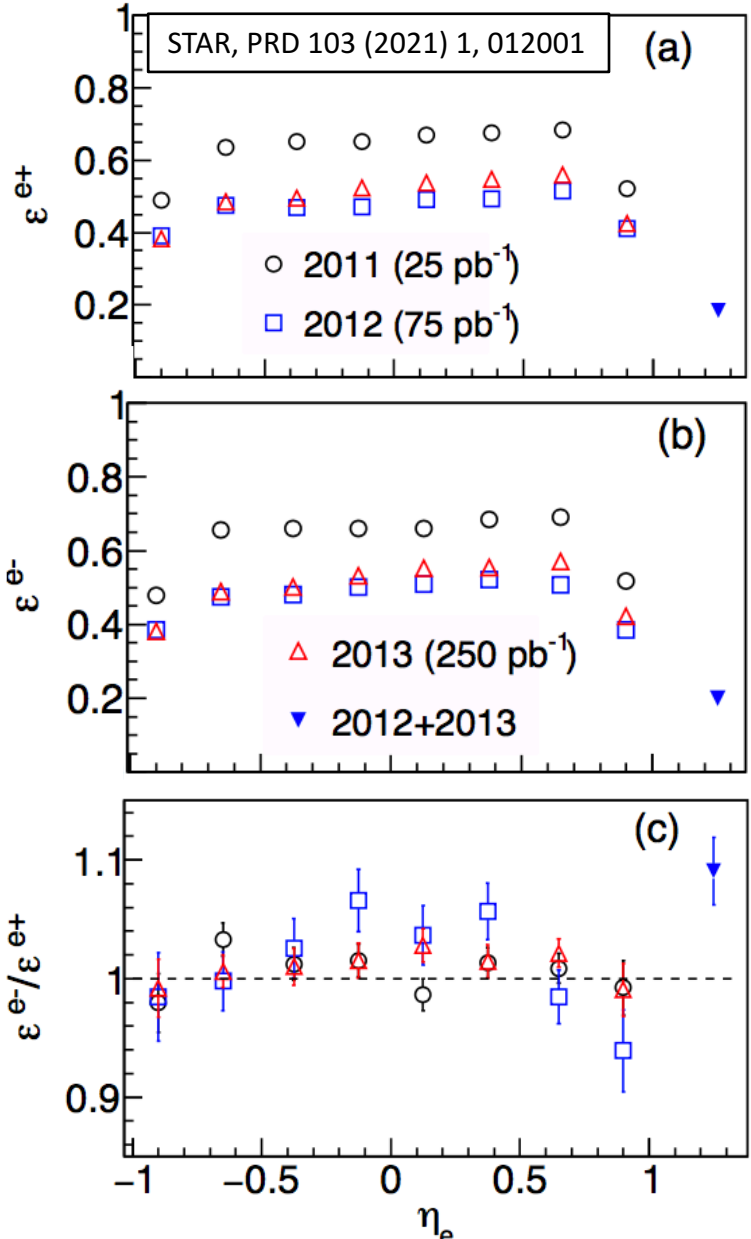
# Backgrounds in the barrel



- Electroweak ( $N_{Z \rightarrow ee}$ ,  $N_{W \rightarrow \tau \nu}$ )
  - Z decays with one unidentified electron
  - Leptonic decay of  $\tau^W$
  - Estimated with MC (Pythia)
- QCD background
  - Due to the limited acceptance and kinematic coverage, imbalance in  $p_T$  may appear in QCD events.
  - Two methods employed to estimate their contributions:
    - Second EEMC ( $N_{EEMC}$ )
      - Accounts for missing backward coverage ( $-2 < \eta < -1$ )
      - Estimated by mirroring the effect of existing EEMC in the forward direction.
    - Data-driven QCD ( $N_{QCD}$ )
      - Remaining background contribution that passes the selection process.
      - Distribution obtained by using events that do not pass the  $p_{T,bal}$ .



# Efficiencies in the barrel



- In the  $W$  cross-section ratio measurement, the expression of the ratio reduces to:

$$\sigma_{W^+}/\sigma_{W^-} = \frac{N_{obs}^+}{\epsilon^+ \int L dt} / \frac{N_{obs}^-}{\epsilon^- \int L dt}$$

$$= \frac{\epsilon^-}{\epsilon^+} \cdot \frac{N_{sig}^+ - N_{bg}^+}{N_{sig}^- - N_{bg}^-}$$

- where  $\epsilon$  represents the product of the efficiencies of our selection process.

$$\epsilon = \epsilon_{trigger} \times \epsilon_{vertex} \times \epsilon_{tracking} \times \epsilon_{tagging}$$

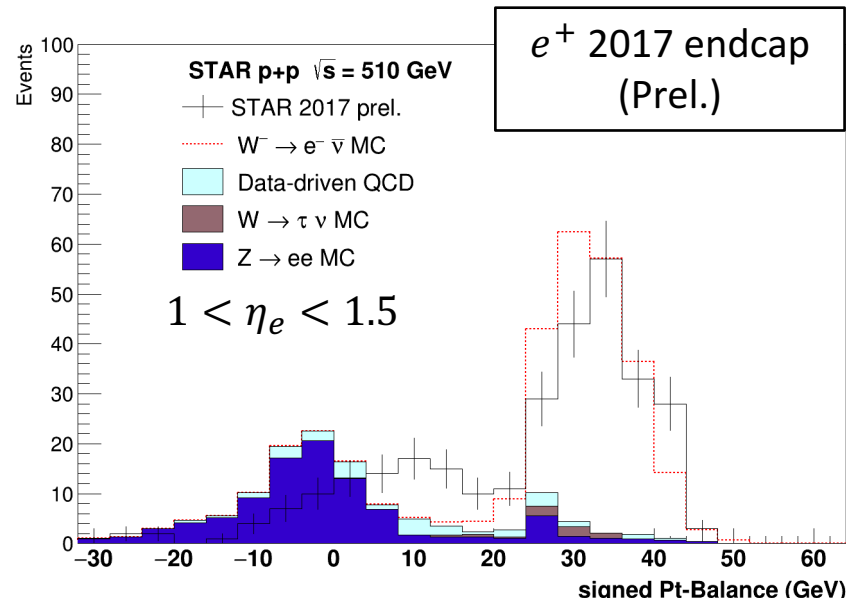
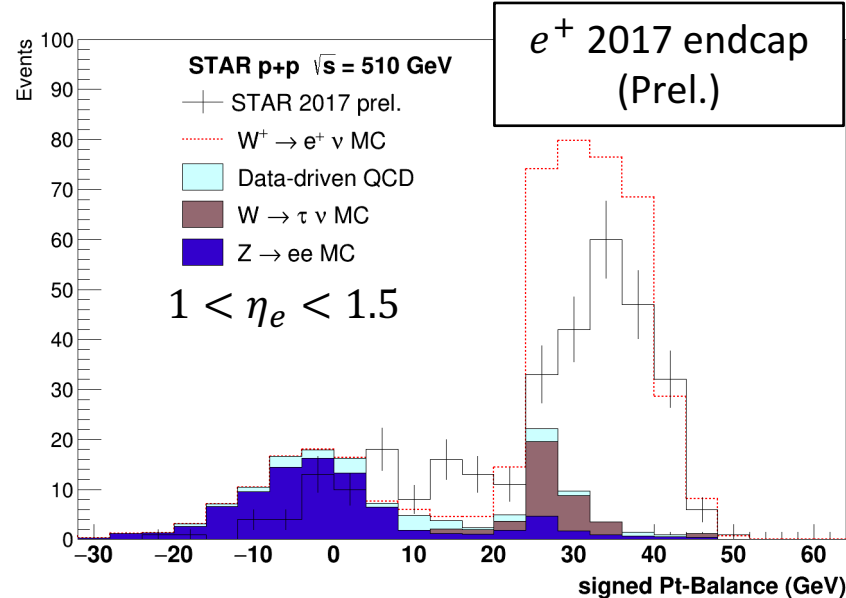
- Lower efficiency in Run 2012 and 2013 (compared to Run 2011) due to higher material deposits.

- Higher tracking efficiency in 2013 than in 2012 due to improvements in tracking algorithm.

- MC study suggests that the efficiency ratio  $\epsilon^-/\epsilon^+$  is consistent with unity and the deviation from unity is taken as a source of systematic uncertainty.



# Endcap measurement

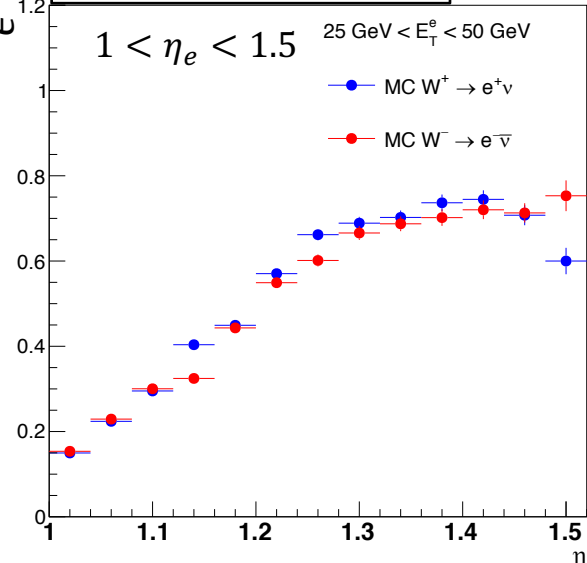


- $W$  tagging method in the endcap region is similar to that for the barrel region.
  - Relaxed tracking requirements.
  - Employ EMC and its subcomponents instead of BEMC.
- Background description also follows a similar procedure.
  - Simulations are used to estimate electroweak background.
  - Description of QCD background purely relies on data-driven method.
- Mismatch in signed- $p_{T,bal} < 20$  GeV due to suboptimal QCD background description.
  - Effect taken as a systematic uncertainty.
  - To be improved in the final measurement.

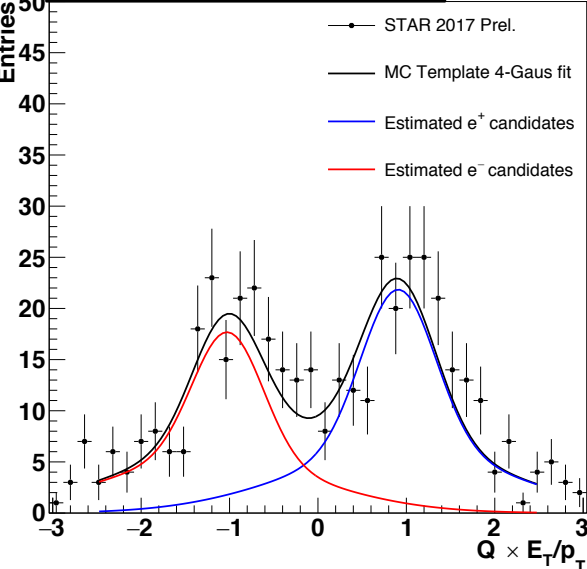


# Endcap corrections

STAR 2017 (endcap)



STAR 2017 (endcap)



- Efficiency correction

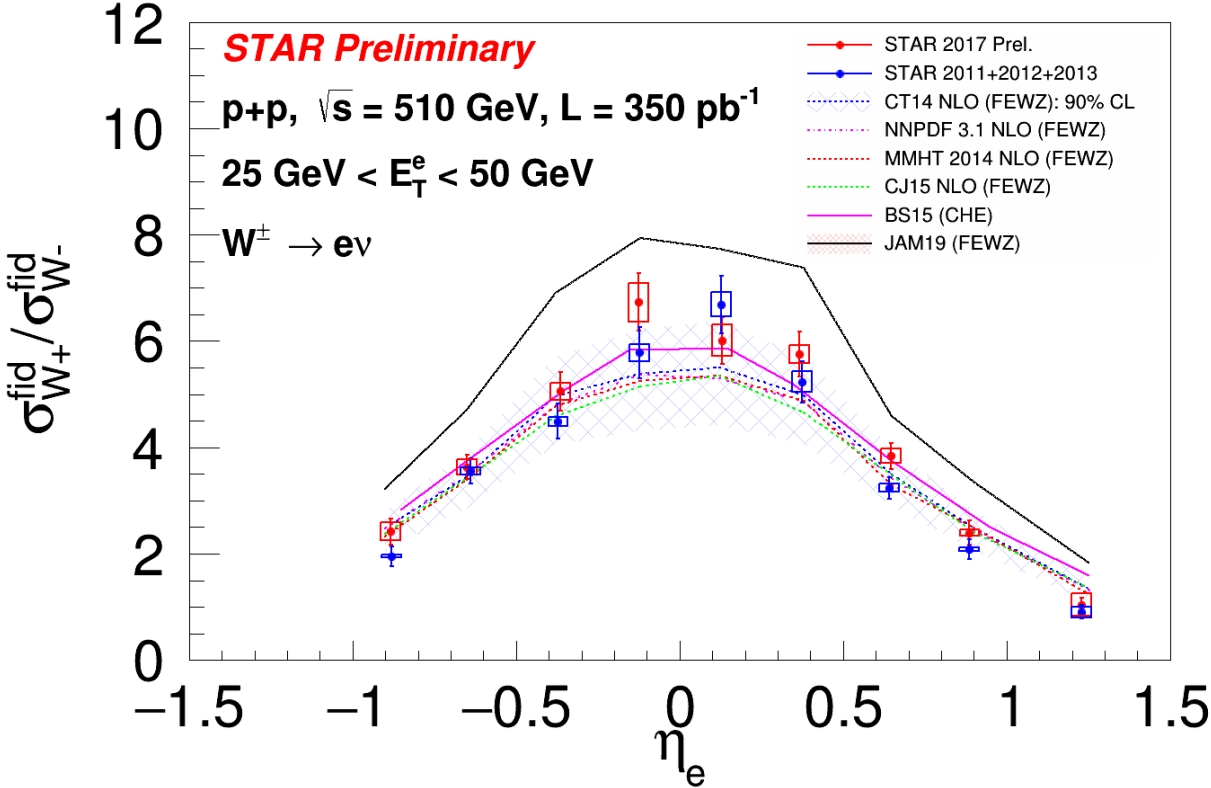
- Evaluates detector acceptance & efficiency of the selection process.
- Considers  $e^W$  within  $25 \text{ GeV} < E_T < 50 \text{ GeV}$ .
- Reduced efficiency in the lower  $\eta$  region due to detector acceptance effect.
- The correction factor ( $\epsilon^- / \epsilon^+$ ) is consistent with unity.
- Remaining deviation is taken as a contribution to the systematic uncertainty.

- Charge selection

- Uses charge ( $Q \times E_T / p_T$ ) distribution to determine the correct-charge ratio.
- Two different fit methods used.
  - MC template method uses  $W \rightarrow e\nu$  simulations for baseline description of the charge fit (nominal).
  - Log-likelihood fitting of double-gaussian function to data.
- Difference between the two results are taken as a contribution to the systematic uncertainty.



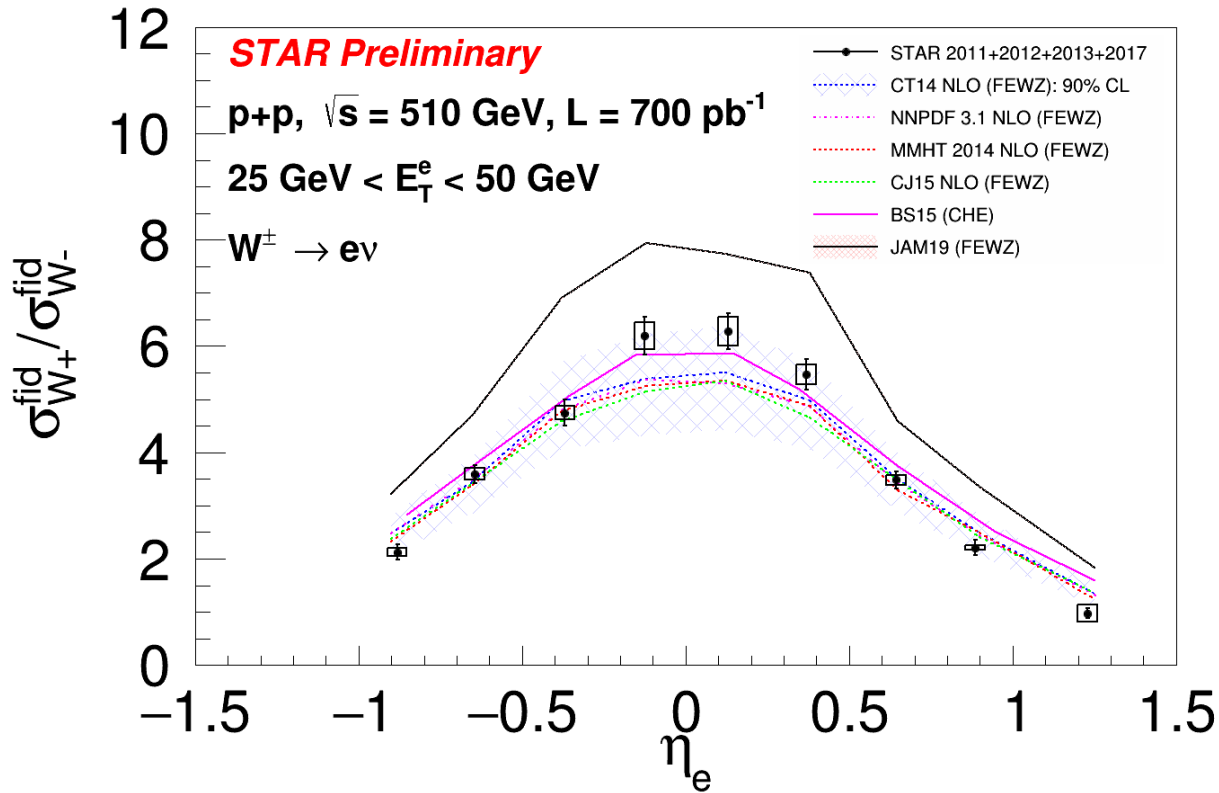
# Results



- Measurement with STAR 2011-2013 data set has been published (PRD 103 (2021) 1, 012001).
- Additional data set taken in 2017 has been analyzed and is in preliminary release.
- These measurements are consistent with each other within their uncertainties.



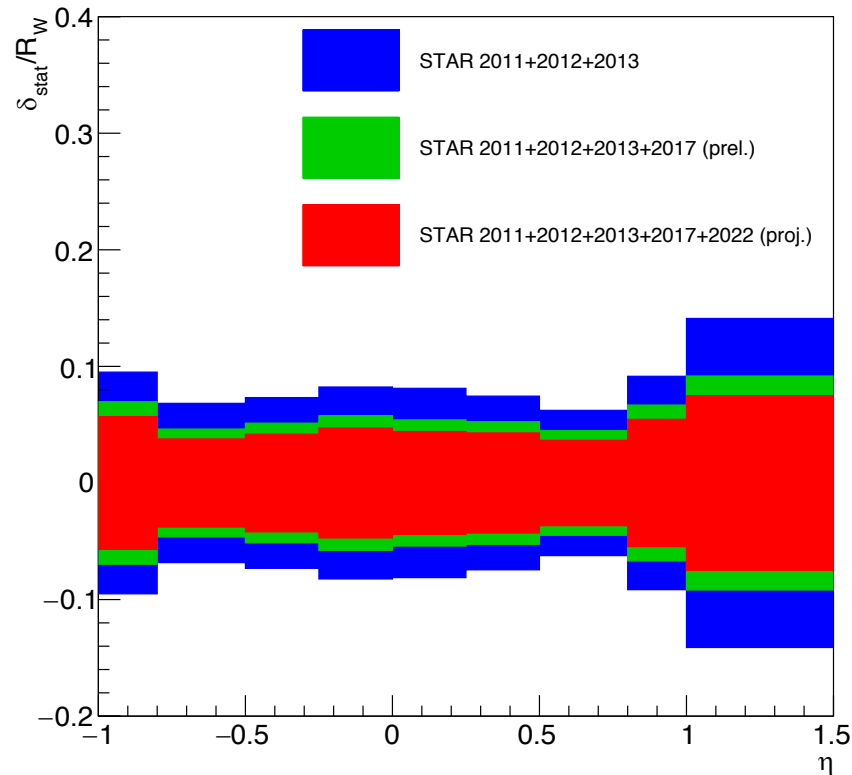
# Results (continued)



- Shown here is the result from the combined STAR 2011-2013 + 2017 data set.
  - Represents combined statistics of  $L \approx 700 \text{ pb}^{-1}$ .
  - Overall good agreement with the current PDF distributions.



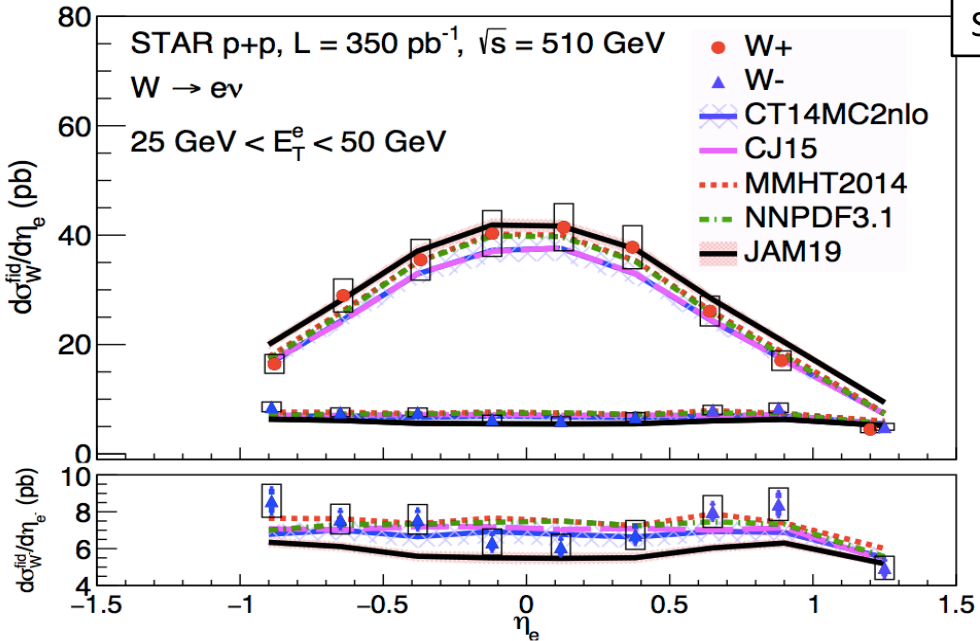
# Results (projection)



- Projection for STAR 2022 data set
  - Combined statistics  $\sim 1 fb^{-1}$
  - Pushes the measurement to the systematic limit.
  - Concludes 500/510 GeV  $pp$  program at STAR

# Absolute cross sections

STAR, PRD 103 (2021) 1, 012001

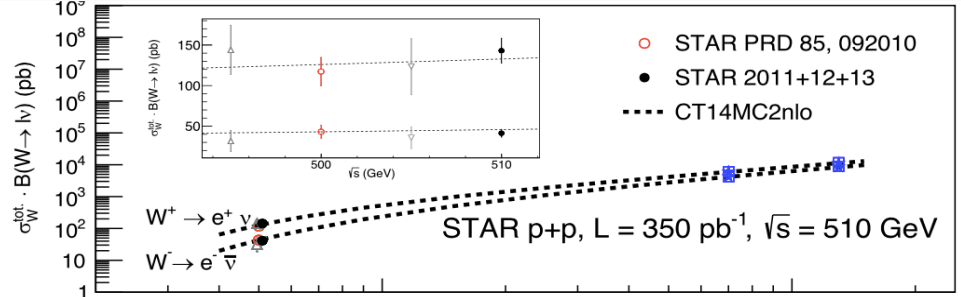


- Measurement of the total cross sections.

$$\sigma_{W/Z}^{fid} = \frac{N_{sig} - N_{bg}}{\epsilon \int L dt}$$

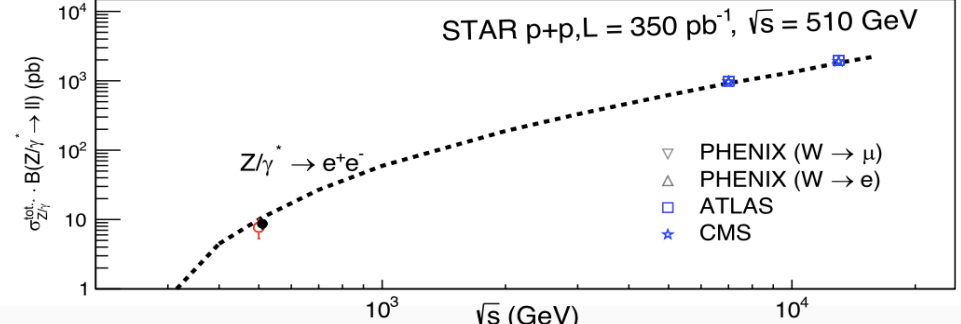
$$\sigma_{W/Z}^{tot} = \sigma_{W/Z}^{fid} / A_{W/Z}$$

- Acceptance correction on 2011 sample ( $\sqrt{s} = 500 \text{ GeV}$ ) to match 2012 and 2013 samples ( $\sqrt{s} = 510 \text{ GeV}$ ) by using FEWZ [PRD 86 (2012) 094034].



## Z reconstruction

- The leptonically decaying  $Z \rightarrow e^+e^-$  bosons are tagged by looking for electron-positron pairs.
- Additional selection process based on the reconstructed mass  $M_Z$  to reject  $\gamma^* \rightarrow e^+e^-$  processes.

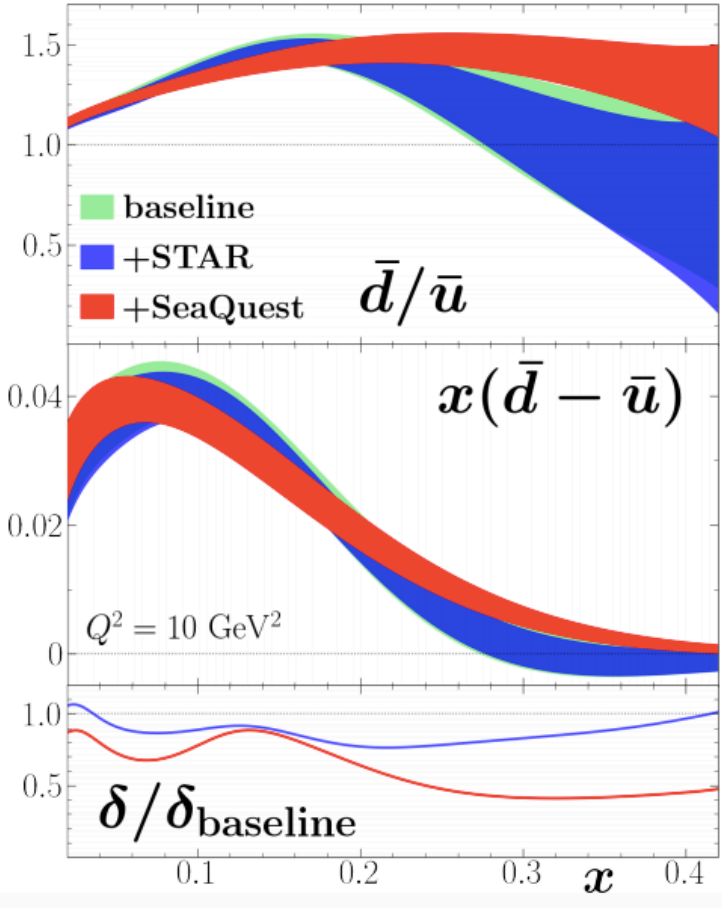


- Results with STAR 2017 in progress.

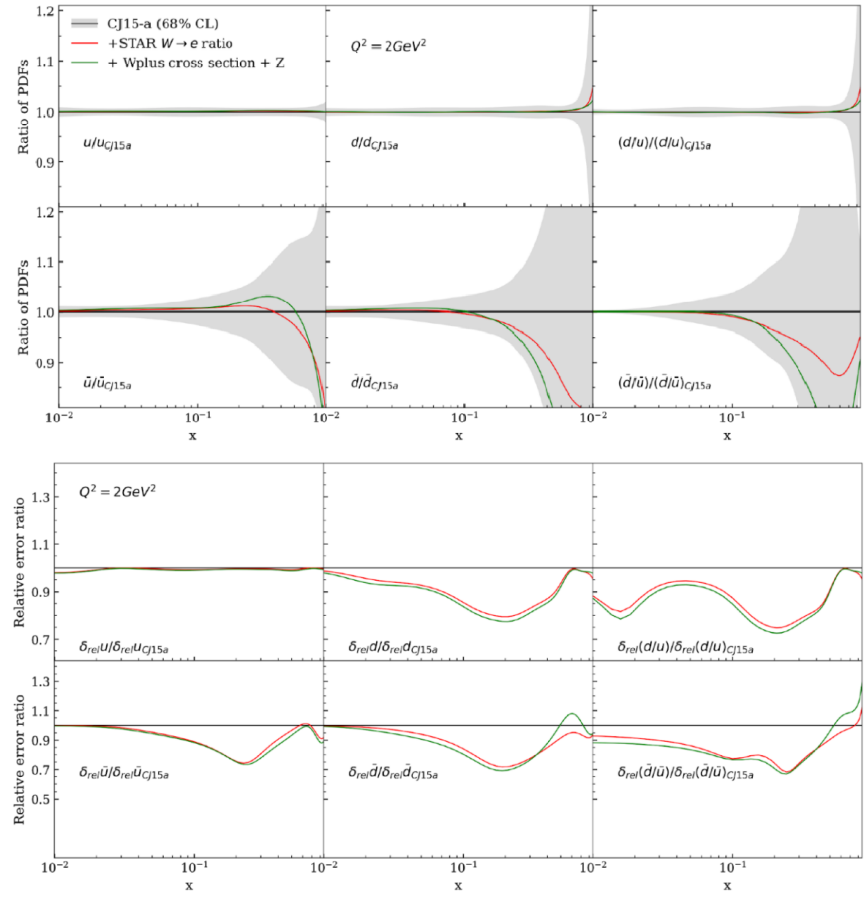


# PDF impacts

JAM, PRD 104 (2021) 7, 074031



S.Park, DIS2021



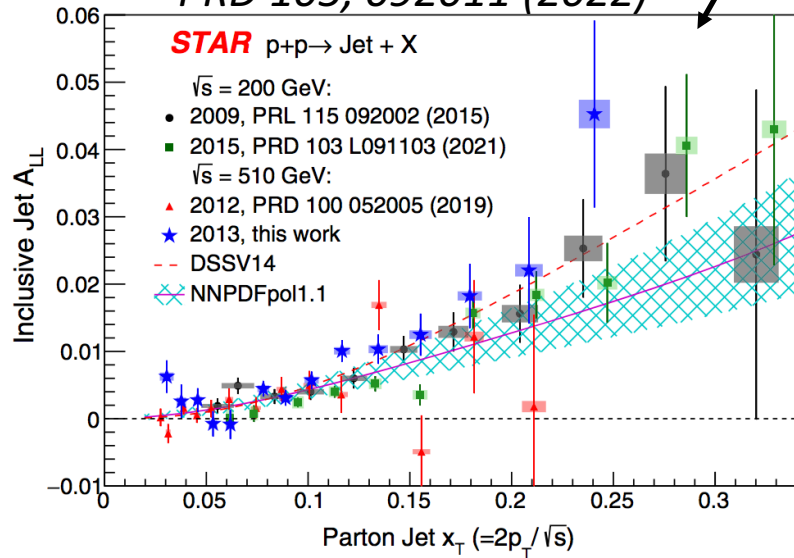
- Recent publication (STAR 2011+2012+2013) has been included in recent global fits.
- STAR data have a moderate amount of impact on the sea quark distributions around  $x \sim 0.2$ .



# Jets at STAR

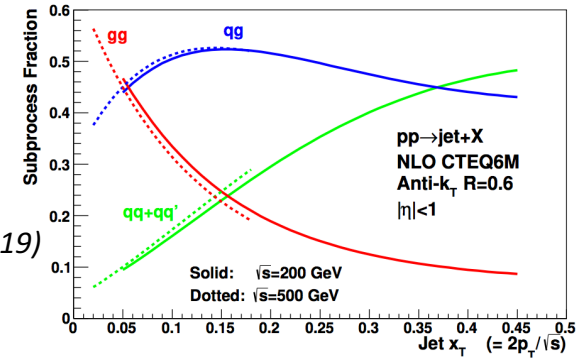
Inclusive jet  $A_{LL}$  with longitudinally-polarized  $pp$  at STAR

PRD 105, 092011 (2022)



- Inclusive jets are used at STAR to extract the gluon helicity distribution  $\Delta g$  via jet  $A_{LL}$  measurements.

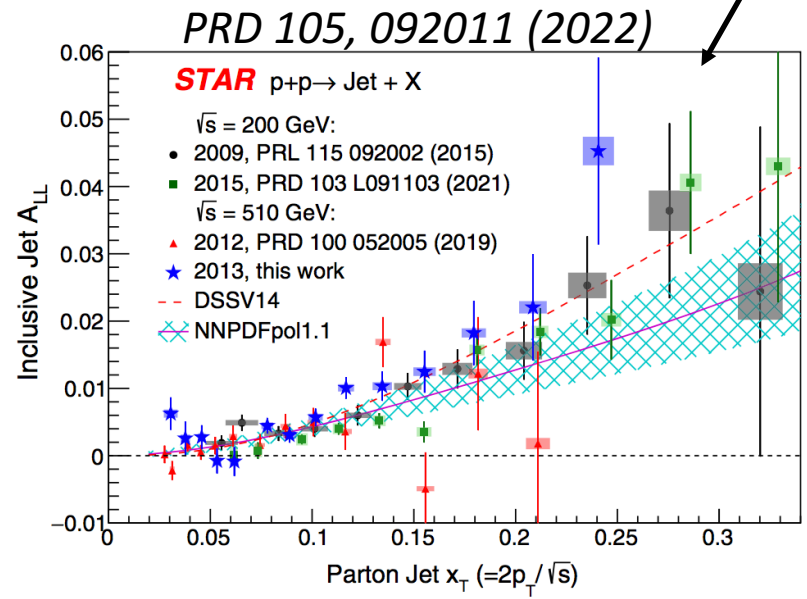
- $A_{LL} \sim \Delta f_1 \otimes \Delta f_2 \otimes \Delta \hat{\sigma}$
- Two different energy modes probe different regions in  $x$ .



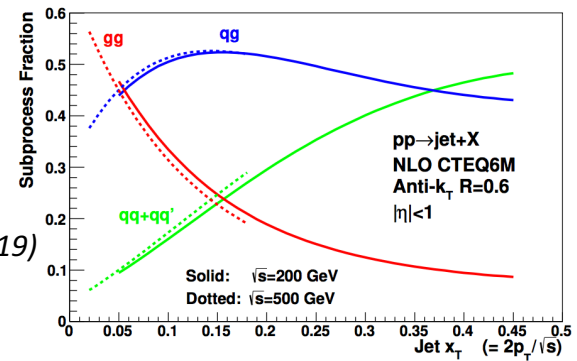
STAR, PRD 100 (2019)  
 5, 052005

# Jets at STAR

Inclusive jet  $A_{LL}$  with longitudinally-polarized  $pp$  at STAR



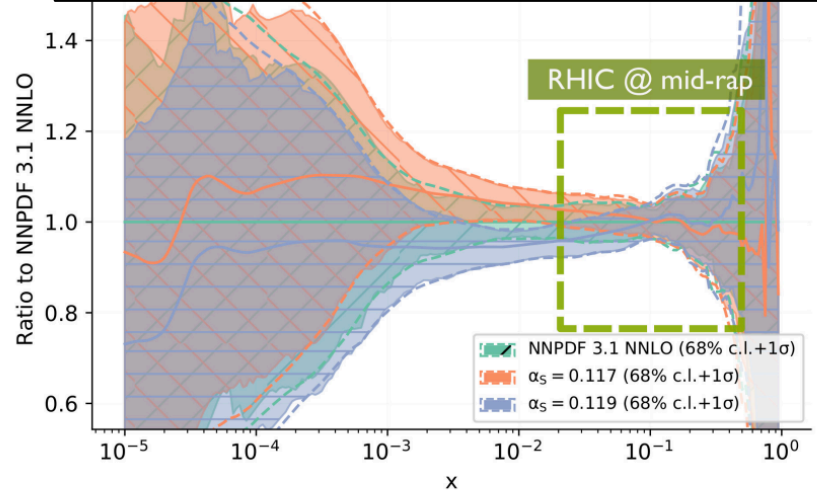
- Inclusive jets are used at STAR to extract the gluon helicity distribution  $\Delta g$  via jet  $A_{LL}$  measurements.
  - $A_{LL} \sim \Delta f_1 \otimes \Delta f_2 \otimes \Delta \hat{\sigma}$
  - Two different energy modes probe different regions in  $x$ .



STAR, PRD 100 (2019) 5, 052005

- Measurements of jets at STAR can be extended to the unpolarized collisions, constraining high- $x$  behavior of gluon PDFs.
  - $d\sigma \sim f_1 \otimes f_2 \otimes d\hat{\sigma}$
  - May also serve as a normalization for other measurements, e.g., hadron fragmentation within jets.

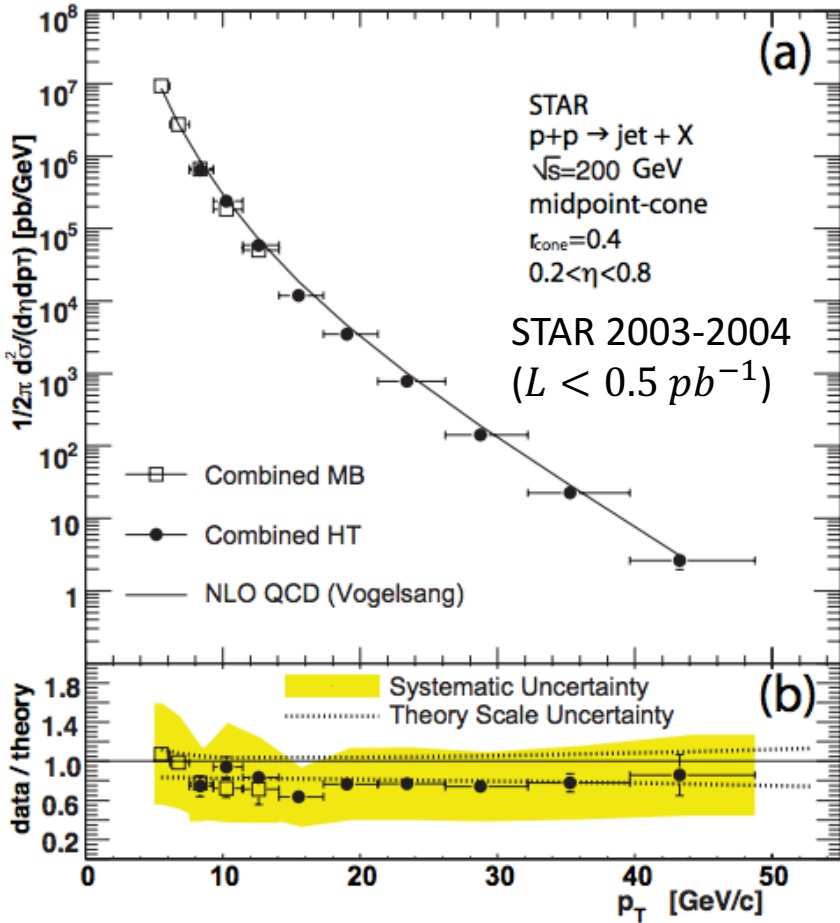
Unpolarized  $g(x, Q^2)$  at  $Q = 2 \text{ GeV}$



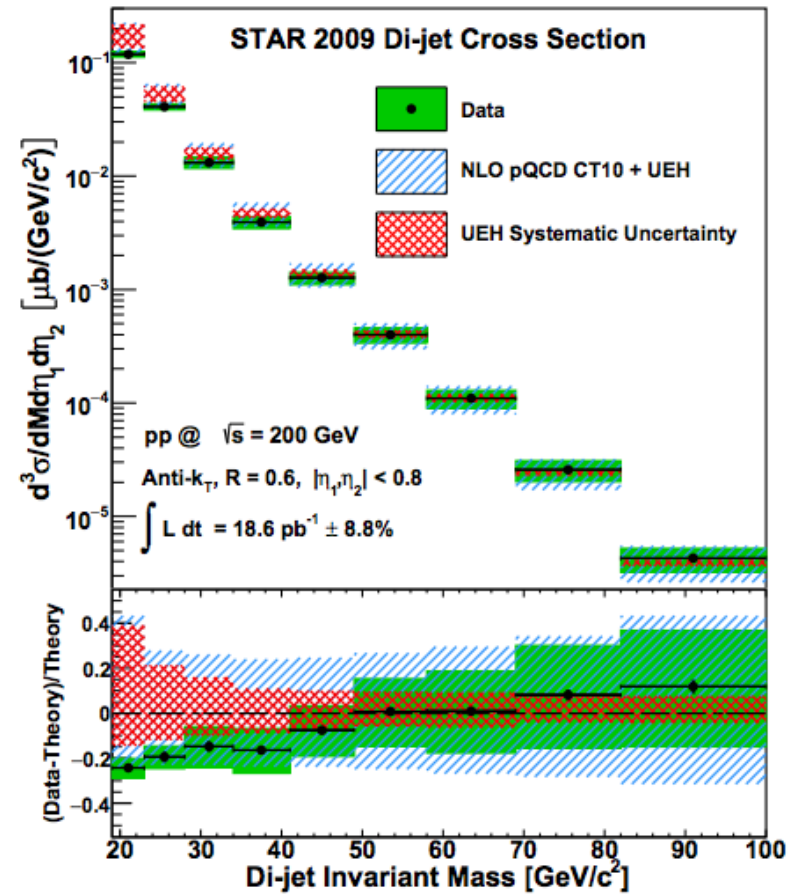
Original plot from NNPDF 3.1 Catalog of plots:  $\alpha_s$  variations at NNLO



# Previous STAR measurements



Phys. Rev. Lett. 97 (2006) 252001

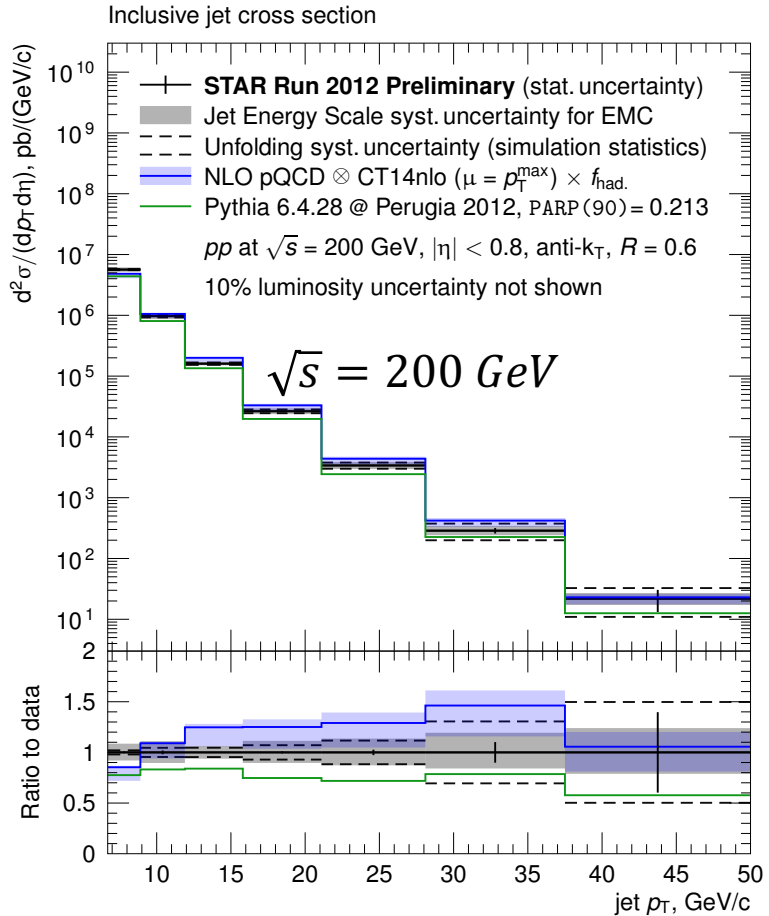


Phys Rev D 95 (2017) 071103

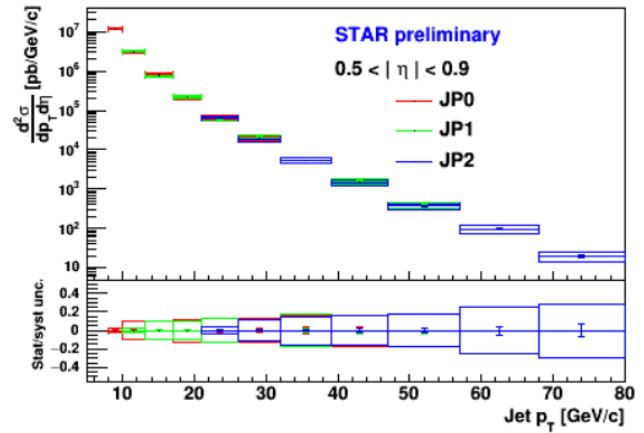
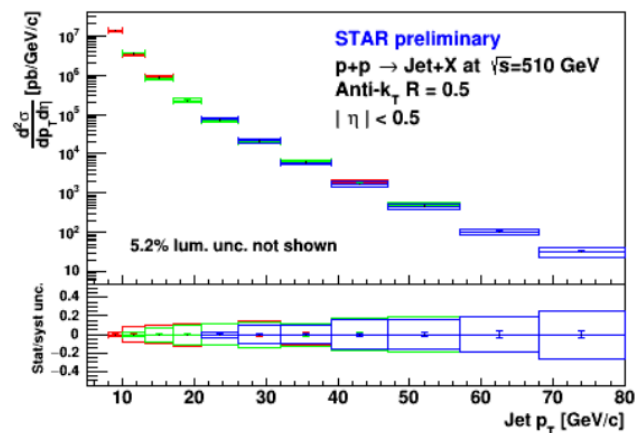
- Inclusive jet cross sections have been measured at STAR with  $pp \sqrt{s} = 200 \text{ GeV}$  beams.
- Previous STAR measurements exist, but suffer from small statistics and high systematic uncertainty due to underlying events.



# Recent measurements of Inclusive Jet



- New results feature  $pp \sqrt{s} = 200 \text{ GeV}, 510 \text{ GeV}$  datasets taken from 2012, corresponding to  $L \approx 20 \text{ pb}^{-1}, 40 \text{ pb}^{-1}$ , respectively.



- Underlying events have been corrected for by estimating shifts in jet  $p_T$  based on the activities around the region off-axis to the jet cone.



# Summary

- $W^+ / W^-$  cross-section ratio has been measured with STAR  $pp \sqrt{s} = 500, 510 \text{ GeV}$  datasets.
  - Probe  $\bar{d}/\bar{u}$  asymmetry in the proton sea, complementary to Drell-Yan measurements.
  - Results based on STAR 2011+2012+2013 ( $L \approx 350 \text{ pb}^{-1}$ ) have been published.
  - STAR 2017 (adds additional  $L \approx 350 \text{ pb}^{-1}$ ) dataset in preliminary state.
  - Combined results consistent to the current PDF distributions
  - Global fit analyses confirm constraining power in the valence region.
- Inclusive Jet cross sections have been measured with both STAR  $pp \sqrt{s} = 200, 510 \text{ GeV}$  datasets.
  - Provide constraints to unpolarized gluon PDF at  $0.01 < x < 0.5$ .
  - Provide normalization for future fragmentation measurements at STAR.
  - Improvements made from the previous measurements due to higher statistics and reduced systematic uncertainty from underlying events.

